Measurement of the Branching Ratio of $K_L \to e^+e^-\gamma\gamma$

T. Nakaya and T. Yamanaka
Department of Physics, Osaka University, Toyonaka, Osaka 560, Japan

K. Arisaka, D. Roberts,* W. Slater, and M. Weaver
University of California at Los Angeles, Los Angeles, California 90024

R. A. Briere, E. Cheu, D. A. Harris,† K. S. McFarland,‡ A. Roodman, B. Schwingenheuer, S. V. Somalwar,§
Y. W. Wah, B. Winstein, and R. Winston
The Enrico Fermi Institute, The University of Chicago, Chicago, Illinois 60637

A. R. Barker
University of Colorado, Boulder, Colorado 80309

E. C. Swallow
Elmhurst College, Elmhurst, Illinois 60126
and The Enrico Fermi Institute, The University of Chicago, Chicago, Illinois 60637

G. J. Bock, R. Coleman, M. Crisler, J. Enagonio, R. Ford, Y. B. Hsiung,
D. A. Jensen, E. Ramberg, and R. Tschirhart
Fermi National Accelerator Laboratory, Batavia, Illinois 60510

E. M. Collins and G. D. Gollin
University of Illinois, Urbana, Illinois 61801

P. Gu, P. Haas, W. P. Hogan, S. K. Kim,‖ J. N. Matthews, S. S. Myung,‖
S. Schnetzer, G. B. Thomson, and Y. Zou
Rutgers University, Piscataway, New Jersey 08855
(Received 2 June 1994)

A new measurement of the $K_L \to e^+e^-\gamma\gamma$ branching ratio was carried out in Fermilab experiment E799. We observed 58 $K_L \to e^+e^-\gamma\gamma$ events. The measured branching ratio is $B(K_L \to e^+e^-\gamma\gamma, E^*_\gamma > 5\ \text{MeV}) = [6.5 \pm 1.2(\text{stat}) \pm 0.6(\text{syst})] \times 10^{-7}$.

PACS numbers: 13.20.Eb, 13.40.Ks

The process $K_L \to e^+e^-\gamma\gamma$ is dominated by a K_L Dalitz decay, $K_L \to e^+e^-\gamma$, with an internal bremsstrahlung photon. This radiative K_L Dalitz decay provides an excellent testing ground for QED radiative corrections. These radiative corrections are particularly important for the precise measurement of the branching ratio of the parent $K_L \to e^+e^-\gamma$ decay, and for studies of the nontrivial $K_L\gamma^*\gamma$ vertex [1] which contributes to the $K_L \to e^+e^-\gamma$ form factor. In addition, the radiative K_L Dalitz decay is expected to be the most serious background [2] in experiments searching for the CP violating decay $K_L \to \pi^0e^+e^-$ [3] beyond the current experimental sensitivity ($\sim 10^{-9}$) [4]. The expected $K_L \to e^+e^-\gamma\gamma$ branching ratio is calculated to be 5.8×10^{-7} with an infrared cutoff of 5 MeV in the center of mass frame of the kaon [2]. The previous measurement of $B(K_L \to e^+e^-\gamma\gamma) = (6.6 \pm 3.2) \times 10^{-7}$ is based on 17 ± 8 events [5]. It is important to measure this branching ratio more precisely to compare it with the expected branching ratio and to better establish the background level for $K_L \to \pi^0e^+e^-$.

The goal of Fermilab experiment E799 was to search for the decay $K_L \to \pi^0e^+e^-$ and other multibody rare K_L decays. Two nearly parallel K_L beams were produced by an 800 GeV proton beam that struck a beryllium target. After collimation the neutral beams entered the detector volume where decays were selected in the interval between 90 and 160 m from the target. A detailed description of the E799 detector can be found elsewhere [6]. Only elements of the detector used in this analysis are described here. The trajectories and momenta of charged tracks were measured with a spectrometer composed of four drift chambers and an analyzing magnet with a nominal 200 MeV/c transverse momentum kick. Each drift chamber had two horizontal and vertical planes, with a typical position resolution of 100 μm per plane. The momentum resolution was $(\sigma_p/p)^2 = (5 \times 10^{-3})^2 + \{1.4 \times 10^{-4}[p(\text{GeV}/c)]\}^2$. The energy and position of electrons and photons were measured with a lead-glass calorimeter composed of 804 blocks arranged in a circular array of 1 m radius with two beam holes in the center to allow the passage of the neutral kaon beams. Each block in the array was $(5.8\ \text{cm})^2 \times 18.7$ radiation lengths deep. The energy resolution of electrons was typically 4.4% for this data sample. The detector had two scintillator hodoscopes

0031-9007/94/73(16)/2169(4)$06.00

between the downstream end of the spectrometer and the calorimeter, which were used for triggering. The detector also had a photon veto system used to reject events in which photons missed the calorimeter.

Two types of triggers were used for this analysis to accept both $K_L \to e^+e^-\gamma\gamma$ and $K_L \to e^+e^-\gamma$ decays. The latter decay mode is used to normalize to the total kaon flux of the experiment. Both triggers required two hits in each hodoscope, drift chamber hits consistent with two tracks, and no veto counter hits. In addition, to satisfy the $K_L \to e^+e^-\gamma\gamma$ trigger there had to be a minimum total energy in the calorimeter of 55 GeV, and four clusters of energy in the calorimeter, each cluster having an energy threshold of 2.5 GeV. Likewise, the $K_L \to e^+e^-\gamma$ trigger demanded a minimum total energy of 6 GeV and three identified clusters, and was prescaled by 14. The energy threshold for the latter trigger was set lower to search for other decay modes. The same energy threshold was used for both samples in the off-line analysis.

Off-line analysis of the data required two reconstructed tracks, each pointing to a cluster, which formed a good vertex in the detector volume. Electrons were identified by requiring the track momentum to match the calorimeter cluster energy to within 15%. Clusters not associated with tracks were considered as photon candidates. The transverse profile of each cluster was required to be consistent with that of a single electromagnetic shower. Events with exactly one (two) photon candidate(s) were used for the $K_L \to e^+e^-\gamma$ ($K_L \to e^+e^-\gamma\gamma$) sample. Kinematic quantities were then calculated assuming the photons in the event originated from the two-track vertex. Events with the square of the transverse momentum of $e^+e^-\gamma\gamma$ with respect to the K_L direction (P_t^2) less than 1000 $(\mathrm{MeV}/c)^2$ were kept. Monte Carlo simulation predicts that this cut keeps 90% of the $K_L \to e^+e^-\gamma\gamma$ signal. The $\pi^+\pi^-\gamma\gamma$ invariant mass ($M_{\pi\pi\gamma\gamma}$) was calculated by assuming that charged particles were pions, and events with this mass between 450 and 550 MeV/c^2 were rejected as $K_L \to \pi^+\pi^-\pi^0$ events. The acceptance loss for the decay $K_L \to e^+e^-\gamma\gamma$ was negligible.

At this stage three remaining background sources contribute to the $M_{ee\gamma\gamma}$ mass window, $466 \le M_{ee\gamma\gamma} \le 530\ \mathrm{MeV}/c^2$ (2.3σ as determined from the Monte Carlo simulation). The first background comes from $K_L \to 2\pi^0$ decays where one π^0 Dalitz decay ($\pi^0 \to e^+e^-\gamma$) and one photon is lost or merges with other photons in the calorimeter ($K_L \to \pi^0\pi_D^0$). The second background results from misidentifying the pion as an electron in $K_L \to \pi e\nu$ decays with two extra photons from bremsstrahlung and accidental processes [$K_{e3}(2\gamma)$]. The third background is $K_L \to e^+e^-\gamma$ decays with an external bremsstrahlung photon or accidental activity [$K_L \to e^+e^-\gamma(\gamma)$].

In order to remove the $K_{e3}(2\gamma)$ background events we define the quantity

$$\min\Sigma\cos = \mathrm{Minimum}(\cos\theta_{11} + \cos\theta_{21}, \cos\theta_{12} + \cos\theta_{22}),$$

where θ_{ij} is the angle between the ith electron and the jth photon in the center of mass frame of the kaon. This quantity distinguishes between Dalitz decays and $K_{e3}(2\gamma)$ decays since one of the photons in a Dalitz decay is usually emitted nearly opposite to the e^+e^- momentum. For $K_{e3}(2\gamma)$ decays, the angles between the photons and the two charged particles are less correlated. Figure 1 shows the $\min\Sigma\cos$ distributions for both the data and the Monte Carlo simulation for $K_L \to e^+e^-\gamma\gamma$ and the major backgrounds. The Monte Carlo simulation consists of generated events overlaid with "accidental events" which correctly sampled the accidental activity in the detector. The $K_L \to e^+e^-\gamma(\gamma)$ background is included in $K_L \to e^+e^-\gamma\gamma$ events: both kinds of events have similar $\min\Sigma\cos$ distributions. In Fig. 1 the $\min\Sigma\cos$ of $K_L \to e^+e^-\gamma\gamma$ events is peaked near -2, well separated from the $K_{e3}(2\gamma)$ events. The $\min\Sigma\cos$ is required to be less than -0.6 in order to reject the $K_{e3}(2\gamma)$ background. This cut removes 93% of the $K_{e3}(2\gamma)$ background while decreasing the $K_L \to e^+e^-\gamma\gamma$ acceptance by 9%.

Another kinematic variable used to reject background is the minimum θ_{ij} angle ($\theta_{\min}$) defined above. The bremsstrahlung photon tends to be emitted in the same direction as the parent electron with a $\theta_{\min}$ of order 10^{-1} rad. In addition, the $\theta_{\min}$ distribution can distinguish between internal and external bremsstrahlung since the distribution for external bremsstrahlung is peaked more sharply near 0. Figure 2 shows the $\theta_{\min}$ distribution of data and Monte Carlo events after the $\min\Sigma\cos$ cut. The value of $\theta_{\min}$ is required to be larger than 0.06 rad to suppress the $K_L \to e^+e^-\gamma(\gamma)$ background, and required to be smaller than 0.5 rad mainly to suppress the $K_L \to \pi^0\pi_D^0$ background. This cut removes 87% of the $K_L \to e^+e^-\gamma(\gamma)$ background and 98% of the $K_L \to \pi^0\pi_D^0$ background while decreasing the $K_L \to e^+e^-\gamma\gamma$ acceptance by 60%.

Figure 3 shows the invariant mass distribution of the $e^+e^-\gamma\gamma$ and $e^+e^-\gamma$ events. The $e^+e^-\gamma$ events were se-

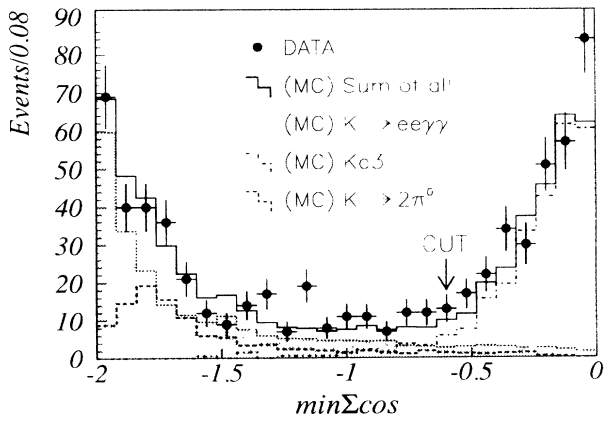

FIG. 1. The $\min\Sigma\cos$ distributions of the data and the Monte Carlo simulation. The level of the background Monte Carlo simulation was estimated by normalizing to the region of reconstructed kaon mass below the K_L mass.

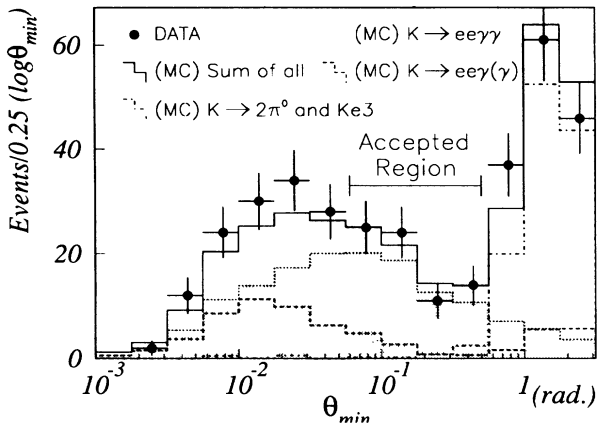

FIG. 2. The minimum angle distribution ($\theta_{\min}$) between each electron, photon combination in the center of mass frame of the kaon. The normalization between the different Monte Carlo samples was based on the Monte Carlo prediction.

lected with the same cuts as the $e^+e^-\gamma\gamma$ events except for the $M_{\pi\pi\gamma\gamma}$ and the $\theta_{\min}$ cuts. There is a clear peak in Fig. 3 at the kaon mass with 69 and 275 events in the kaon mass window for the $e^+e^-\gamma\gamma$ and $e^+e^-\gamma$ events, respectively. The background in the $e^+e^-\gamma\gamma$ sample consists of $K_L \to \pi^0\pi^0_D$, $K_{e3}(2\gamma)$, $K_L \to \pi^0\pi^0\pi^0_D$, and $K_L \to e^+e^-\gamma(\gamma)$ events. Other background sources such as $K_L \to \pi^+\pi^-\pi^0$, $K_L \to \pi^0_D\pi^0_D$, and $K_L \to \pi^0\pi^0_D\pi^0_D$ were negligible. We used the Monte Carlo simulation to estimate the levels of the first three sources of background. Using the reconstructed kaon mass we normalized each background to the region below the K_L mass and extrapolated the number we expect in the K_L mass window. The number of background events is 2.1 ± 0.3 events from $K_L \to \pi^0\pi^0_D$, 0.6 ± 0.2 events from $K_{e3}(2\gamma)$, and 0.5 ± 0.2 events from $K_L \to \pi^0\pi^0\pi^0_D$. The background to $e^+e^-\gamma$ events comes from $K_{e3}(\gamma)$ decays, and

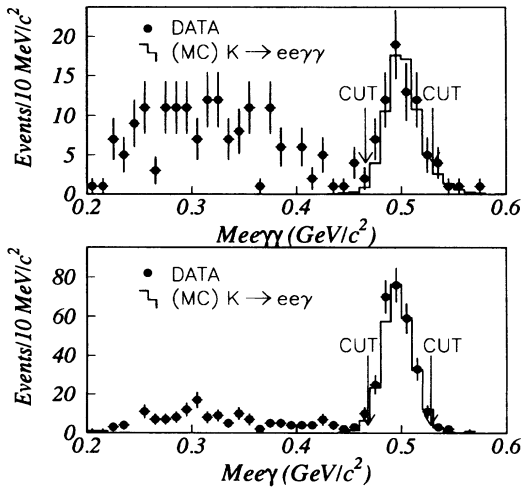

FIG. 3. The invariant mass distributions of $e^+e^-\gamma\gamma$ events and $e^+e^-\gamma$ events.

the number was estimated to be 2.3 ± 0.9. Correcting for these backgrounds reduces the number of $e^+e^-\gamma\gamma$ ($N_{ee\gamma\gamma}$) and $e^+e^-\gamma$ ($N_{ee\gamma}$) events to 65.8 ± 8.3 events and 272.7 ± 16.6 events, respectively.

In order to determine the $K_L \to e^+e^-\gamma\gamma$ branching ratio, it is necessary to determine the amount of $K_L \to e^+e^-\gamma(\gamma)$ background which remains in the $e^+e^-\gamma\gamma$ sample. In addition, the normalization sample, $e^+e^-\gamma$ events, consists of the radiative K_L Dalitz decay with a missing photon, and the K_L Dalitz decay. We use the following method to disentangle the number of radiative and nonradiative K_L Dalitz decays in the $e^+e^-\gamma\gamma$ and $e^+e^-\gamma$ samples. The ratio of the number of remaining $e^+e^-\gamma\gamma$ events to $e^+e^-\gamma$ events is related to $R = B(K_L \to e^+e^-\gamma\gamma)/B(K_L \to e^+e^-\gamma)$ as

$$\frac{N_{ee\gamma\gamma}}{N_{ee\gamma}} = \frac{(1-R)A_{ee\gamma\to ee\gamma\gamma} + RA_{ee\gamma\gamma\to ee\gamma\gamma}}{(1-R)A_{ee\gamma\to ee\gamma} + RA_{ee\gamma\gamma\to ee\gamma}}, \quad (1)$$

where $B(K_L \to e^+e^-\gamma)$ is the branching ratio of the $K_L \to e^+e^-\gamma$ including the radiative decay, $e^+e^-\gamma\gamma$, and $A_{x\to y}$ is the Monte Carlo probability that an event generated as x is accepted as y. Each acceptance, listed in Table I, was determined from a Monte Carlo simulation with energies of kaons between 35 and 220 GeV. The Monte Carlo generator for $K_L \to e^+e^-\gamma$ and $K_L \to e^+e^-\gamma\gamma$, based on Ref. [7], is divided into two parts by a cutoff parameter for $M_{\gamma\gamma}$. The value of this cutoff is fixed at 2.29 MeV/c^2, the same as in Ref. [7], and it is far below the detector threshold. Above this cutoff, $K_L \to e^+e^-\gamma\gamma$ events were explicitly generated, and below it nonradiative $K_L \to e^+e^-\gamma$ events were generated. In both cases external bremsstrahlung processes were simulated.

By solving Eq. (1), R is found to be 0.29 ± 0.06(stat). By using the numerator of Eq. (1), the number of $K_L \to e^+e^-\gamma\gamma$ events is calculated to be 57.5 ± 8.5(stat), and the number of $K_L \to e^+e^-\gamma(\gamma)$ events is 8.3 ± 2.0(stat). In the normalization sample we calculate the number of $K_L \to e^+e^-\gamma$ events to be 173.5 ± 23.4 and the number of $K_L \to e^+e^-\gamma\gamma$ events to be 99.2 ± 17.0. The calorimeter energy threshold is approximately 10 MeV in the kaon rest frame. An infrared cutoff of 5 MeV ($E^*_\gamma \geq 5$ MeV) is used to calculate the branching ratio of $K_L \to e^+e^-\gamma\gamma$, to allow direct comparison of this measurement to theoretical predictions [2] as well as the previous published measurement [5]. The Monte Carlo simulation predicts the effect of this cutoff to be $B(K_L \to e^+e^-\gamma\gamma, E^*_\gamma \geq 5\ \text{MeV})/B(K_L \to$

TABLE I. The acceptance for each decay mode. The numbers in the $ee\gamma\gamma*$ column are for the less restrictive $ee\gamma\gamma$ analysis as described in the text. The acceptance of observed $ee\gamma$ events includes a trigger prescale factor of 1/14.

	Acceptances (10^{-4})		
Decay mode	$ee\gamma$	$ee\gamma\gamma$	$ee\gamma\gamma*$
$K_L \to ee\gamma$	9.2	0.44	2.8
$K_L \to ee\gamma\gamma$	13.1	7.6	17.2

$e^+e^-\gamma\gamma) = 0.247$. By using the inclusive branching ratio, $B(K_L \to e^+e^-\gamma) = (9.1 \pm 0.5) \times 10^{-6}$ [1], the branching ratio of $K_L \to e^+e^-\gamma\gamma$ is measured to be $B(K_L \to e^+e^-\gamma\gamma, E^*_\gamma \geq 5$ MeV$) = [6.5 \pm 1.2(\text{stat})] \times 10^{-7}$.

The main sources of systematic errors come from uncertainties in normalization, detector resolution, and background. The contribution to the total systematic from the uncertainty in the $K_L \to e^+e^-\gamma$ branching ratio is 5.5%. Uncertainties in the position resolution of extra clusters in the calorimeter introduce a systematic error through the $\theta_{\min}$ cut. The position resolution of extra clusters was estimated from special electron calibration runs in the data to be 5.3 mm, while the Monte Carlo simulation predicted 4.6 mm. This disagreement leads to a 3.3% systematic error. We also found that the cuts used to isolate electromagnetic clusters introduced a systematic error of 2.2%. The total amount of material upstream of the analyzing magnet is 1.16% of a radiation length. Uncertainty in the amount of material can change the estimate of the $K_L \to e^+e^-\gamma(\gamma)$ background level. The emission probability of an external bremsstrahlung photon differed by 20% between the amount found from special calibration run data and the Monte Carlo expectation. This discrepancy results in an additional 3.5% systematic error in the branching ratio. The energy and momentum resolution couple directly into the acceptance calculation and the uncertainty in these values adds an additional 1.5% and 1.0% to the systematic error, respectively. We found that the difference between using phase space and the form factor, α_{K^*}, resulted in a systematic error of 2.2%. The other sources of systematic error were the Monte Carlo statistics, 3.4%, and the background subtraction, 0.7%. The total systematic error was calculated to be 8.8% by adding all individual components in quadrature, leading to a final result of $B(K_L \to e^+e^-\gamma\gamma, E^*_\gamma \geq 5$ MeV$) = [6.5 \pm 1.2(\text{stat}) \pm 0.6(\text{syst})] \times 10^{-7}$.

A less restrictive analysis was performed to check the above result, and to study the kinematic distributions of $K_L \to e^+e^-\gamma\gamma$ events with higher statistics. Removing the $\theta_{\min}$ cut at 0.06 rad increases the number of $e^+e^-\gamma\gamma$ events to 198.8 ± 14.3. This less restrictive analysis gives $B(K_L \to e^+e^-\gamma\gamma, E^*_\gamma \geq 5$ MeV$) = [7.7 \pm 1.4(\text{stat}) \pm 1.0(\text{syst})] \times 10^{-7}$ based on 151.6 ± 17.4 $K_L \to e^+e^-\gamma\gamma$ signals and 47.2 ± 9.9 $K_L \to e^+e^-\gamma(\gamma)$ background events. This result is consistent with the more restrictive analysis. Figure 4 shows the M_{ee} and $M_{\gamma\gamma}$ distributions of the $e^+e^-\gamma\gamma$ events from the less restrictive analysis. The data distributions are consistent with the sum of the $K_L \to e^+e^-\gamma\gamma$ and the $K_L \to e^+e^-\gamma(\gamma)$ phase space Monte Carlo distributions. This is the first time these kinematic distributions were compared for the $K_L \to e^+e^-\gamma\gamma$ decay. In conclusion, we have determined the $K_L \to e^+e^-\gamma\gamma$ branching ratio to be $B(K_L \to e^+e^-\gamma\gamma, E^*_\gamma \geq 5$ MeV$) = [6.5 \pm 1.2(\text{stat}) \pm 0.6(\text{syst})] \times 10^{-7}$. This measurement is more precise than previous measurements, and it is consistent with theoretical expectations.

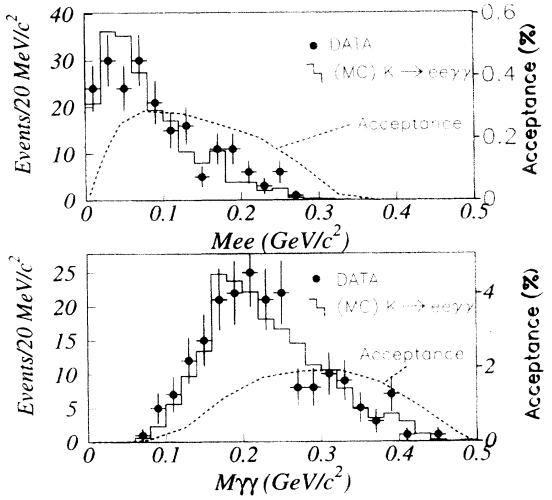

FIG. 4. The e^+e^- invariant mass and the $\gamma\gamma$ invariant mass distributions without the minimum angle cut ($\theta_{\min} \geq 0.06$). The Monte Carlo simulation includes the sum of the $K_L \to e^+e^-\gamma\gamma$ and $K_L \to e^+e^-\gamma(\gamma)$ samples in the proportions described in the text. Also shown is the $K_L \to e^+e^-\gamma\gamma$ acceptance as a function of M_{ee} and $M_{\gamma\gamma}$.

This research was supported by the U.S. National Science Foundation and the U.S. Department of Energy. We would like to thank Greg Makoff, Margherita Vittone, Gene Beck, John Krider, and the staff of the Fermilab accelerator, computing and research divisions. We thank H. B. Greenlee for his help with regard to the $K_L \to e^+e^-\gamma\gamma$ Monte Carlo simulation. One of us (Y.W.W.) would like to acknowledge support from an OJI grant from the DOE. Another of us (T.N.) would like to acknowledge support from JSPS Fellowships.

*Present address: University of California, Santa Barbara, Santa Barbara, CA 93106.
†Present address: University of Rochester, Rochester, NY 14627.
‡Present address: Fermi National Accelerator Laboratory, Batavia, IL 60510.
§Present address: Rutgers University, Piscataway, NJ 08855.
‖Present address: Seoul National University, Seoul 151–742, Korea.

[1] Particle Data Group, K.Hikasa *et al.*, Phys. Rev. D **45**, S1 (1992).
[2] H. B. Greenlee, Phys. Rev. D **42**, 3724 (1990).
[3] J. F. Donoghue, B. R. Holstein, and G. Valencia, Phys. Rev. D **35**, 2769 (1987).
[4] D. A. Harris *et al.*, Phys. Rev. Lett. **71**, 3918 (1993).
[5] W. M. Morse *et al.*, Phys. Rev. D **45**, 36 (1992).
[6] K. S. McFarland *et al.*, Phys. Rev. Lett. **71**, 31 (1993).
[7] L. Roberts and J. Smith, Phys. Rev. D **33**, 3457 (1986).

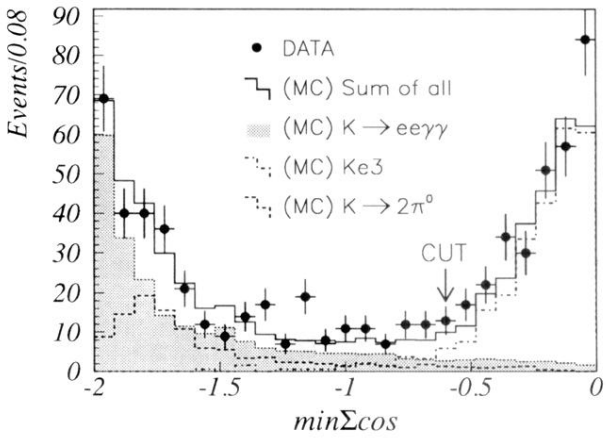

FIG. 1. The minΣ cos distributions of the data and the Monte Carlo simulation. The level of the background Monte Carlo simulation was estimated by normalizing to the region of reconstructed kaon mass below the K_L mass.

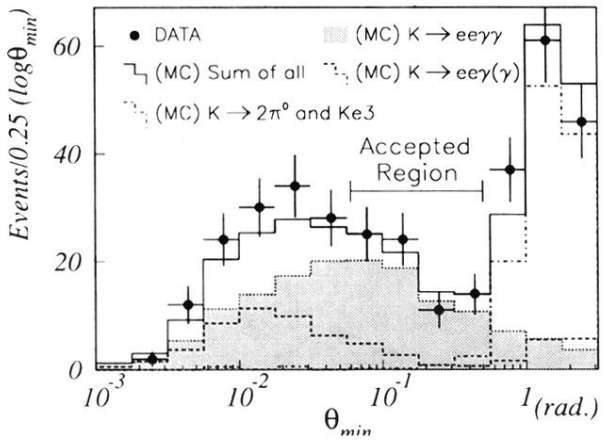

FIG. 2. The minimum angle distribution ($\theta_{\min}$) between each electron, photon combination in the center of mass frame of the kaon. The normalization between the different Monte Carlo samples was based on the Monte Carlo prediction.